NeuroImage: Clinical 20 (2018) 102–109

Contents lists available at ScienceDirect

NeuroImage: Clinical

journal homepage: www.elsevier.com/locate/ynicl

Hyperintense sensorimotor T1 spin echo MRI is associated with brainstem abnormality in chronic fatigue syndrome

Leighton R. Barnden[a,*], Zack Y. Shan[a], Donald R. Staines[a], Sonya Marshall-Gradisnik[a], Kevin Finegan[b], Timothy Ireland[b], Sandeep Bhuta[b]

[a] National Centre for Neuroimmunology and Emerging Diseases, Menzies Health Institute Queensland, Griffith University, Southport, QLD 4222, Australia
[b] Medical Imaging Department, Gold Coast University Hospital, Parklands, QLD 4215, Australia

ARTICLE INFO

Keywords:
Chronic Fatigue Syndrome
Brainstem
Motor
Sensorimotor
T1wSE
Myelin
Upregulation

ABSTRACT

We recruited 43 Chronic Fatigue Syndrome (CFS) subjects who met Fukuda criteria and 27 healthy controls and performed 3T MRI T1 and T2 weighted spin-echo (T1wSE and T2wSE) scans. T1wSE signal follows T1 relaxation rate (1/T1 relaxation time) and responds to myelin and iron (ferritin) concentrations. We performed MRI signal level group comparisons with SPM12. Spatial normalization after segmentation was performed using T2wSE scans and applied to the coregistered T1wSE scans. After global signal-level normalization of individual scans, the T1wSE group comparison detected *decreased* signal-levels in CFS in a brainstem region (cluster-based inference controlled for family wise error rate, $P_{FWE} = 0.002$), and *increased* signal-levels in large bilateral clusters in sensorimotor cortex white matter (cluster $P_{FWE} < 0.0001$). Moreover, the brainstem T1wSE values were negatively correlated with the sensorimotor values for both CFS ($R^2 = 0.31$, $P = 0.00007$) and healthy controls ($R^2 = 0.34$, $P = 0.0009$), and the regressions were co-linear. This relationship, previously unreported in either healthy controls or CFS, in view of known thalamic projection-fibre plasticity, suggests brainstem conduction deficits in CFS may stimulate the upregulation of myelin in the sensorimotor cortex to maintain brainstem – sensorimotor connectivity. VBM did not find group differences in regional grey matter or white matter volumes. We argued that increased T1wSE observed in sensorimotor WM in CFS indicates increased myelination which is a regulatory response to deficits in the brainstem although the causality cannot be tested in this study. Altered brainstem myelin may have broad consequences for cerebral function and should be a focus of future research.

1. Introduction

The chronic fatigue syndrome or myalgic encephalomyelitis (CFS) is a common, debilitating, multisystem disorder of uncertain pathogenesis, for which there exists evidence of dysregulation of the central nervous system, immune system and cellular energy metabolism (Carruthers et al., 2011). Numerous fMRI and connectivity studies in CFS have suggested abnormal WM function (Boissoneault et al., 2016a; Boissoneault et al., 2016b; Caseras et al., 2008; Cook et al., 2007; de Lange et al., 2004; Gay et al., 2016; Kim et al., 2015; Lange et al., 2005; Mizuno et al., 2016; Mizuno et al., 2015; Tanaka et al., 2006; Wortinger et al., 2016; Wortinger et al., 2017; Shan et al., 2018a; Shan et al., 2018b) although they do not inform regarding its biological origin. Here we examine structural scan signal levels that respond to both myelin and iron levels to offer novel insights into WM status in CFS.

Early MRI utilised spin-echo (SE) sequences which yielded T1 and T2 weighted (T1wSE and T2wSE) scans with good signal to noise ratio (SNR) that showed little spatial distortion. Indeed, T1wSE and T2wSE scans still have an important clinical role. The 'weighted' or 'w' here refers to the fact that although T1w levels are primarily determined by local T1 relaxation rate, they are also weakly affected by local T2 relaxation rate. The price paid for the high quality of SE scans is a long

Abbreviations: BA, Brodmann Area; CFS, chronic fatigue syndrome; GM, grey matter; HC, healthy controls; M1, primary motor cortex; P_{FWE}, family-wise error corrected cluster P statistic; PD, Parkinson's Disease; ROI, region of interest; S1, primary somatosensory cortex; SNR, signal to noise ratio; T1wSE, T1 weighted spin echo; TE, echo time; TIV, total intracranial volume; TR, repetition time; VBIS, voxel based iterative sensitivity; VBM, voxel based morphometry; VTA, ventral tegmental area; WM, white matter

* Corresponding author at: National Centre for Neuroimmunology and Emerging Diseases, Menzies Health Institute Queensland, Griffith University, Southport, QLD 4222, Australia.

E-mail addresses: l.barnden@griffith.edu.au (L.R. Barnden), z.shan@griffith.edu.au (Z.Y. Shan), d.staines@griffith.edu.au (D.R. Staines), s.marshall-gradisnik@griffith.edu.au (S. Marshall-Gradisnik), Kevin.Finegan@health.qld.gov.au (K. Finegan), Timothy.Ireland@health.qld.gov.au (T. Ireland).

https://doi.org/10.1016/j.nicl.2018.07.011
Received 4 May 2018; Received in revised form 29 June 2018; Accepted 10 July 2018
Available online 11 July 2018

acquisition time (up to 10 minutes) and limited axial spatial resolution (early axial voxel sizes were 5 mm). In research, T1wSE scans have almost exclusively been replaced by T1w gradient recalled echo (GRE) scans which typically have acquisition times of a few minutes and isotropic voxel sizes of 1 mm or less. Although T1wGRE scans also show better GM to WM contrast, their SNR is poorer than T1wSE and they suffer from significant spatial distortion. T1wSE scans are therefore expected to be more sensitive than T1wGRE for quantitative cross-sectional studies of T1 relaxation effects. Similarly, it is now common to use 'optimised 3D fast-spin-echo' for T2w scans. A selected variable flip-angle profile yields a T2w spin-echo echo signal that is stable for long enough to facilitate 3D (single slab) imaging in shorter scan times (Mugler JP 3rd, 2014). Although the resultant scan has T2 contrast, signal levels also have some T1 dependence (Mugler JP 3rd, 2014). Because of our interest in the brainstem, we chose them for their spin-echo advantages to perform segmentation and spatial normalization, instead of the distortion-prone 3D T1w gradient echo scans. It is not clear whether T2wSE scans from the variable flip angle method have the same contrast dependence on [myelin] and [Fe] as conventional (flip angle 90°) T2wSE scans.

T1w and T2w scans are regarded as 'structural' and quantitative studies based on their signal levels are few. This is mainly because their average signal levels vary considerably from subject to subject due to variable head size and positioning in the scanner. Abbott et al. (2009) have specifically addressed the problem of adjusting for inter-subject variation in global T2wSE in the context of cross-sectional voxel-based studies. Based on a preliminary voxel-based comparison of patient and control groups, they identified a subset of voxels with low inter-subject residual variance, and used its mean voxel value to adjust for inter-subject global variation. They called this method voxel based iterative sensitivity (VBIS) and validated it for T2wSE in a group of patients using T2 relaxometry (Abbott et al., 2009). We demonstrated that VBIS yielded useful clinical information when applied to both T1wSE and T2wSE in a study of CFS (Barnden et al., 2015; Barnden et al., 2011; Barnden et al., 2016). Of particular interest was our T1wSE observation indicating that in CFS, myelination increased with severity in the internal capsule (Barnden et al., 2015).

This motivated us to acquire T1wSE scans here with optimal SNR by choosing not to accelerate them (no turbo). Moreover, the 64 channel head-neck coil of the 3T MRI system used here yielded very high signal to noise ratio (SNR) in cortical GM and shallow WM. A similar 64 channel head-only coil showed that SNR at the brain centre was comparable with a body receive coil (Maubon et al., 1999), increased by a factor of 2 near 30 mm below the cortex and by a factor of 4 in the cortex (Keil et al., 2013). This CFS study therefore offered unprecedented sensitivity to variability in the near-surface gyral myelin that influences T1wSE signals and was optimal for a cross-sectional study to explore relative white matter myelination. The trade-off was an acquisition time of nearly 9 minutes and an axial voxel size of 3 mm.

We detected extended increases in T1wSE in sensorimotor WM in CFS. Decreases in the brainstem in the same scans prompted ROI analysis of relative brainstem and sensorimotor T1wSE levels which revealed an inverse correlation between them that was seen in both healthy controls and CFS.

2. Methods

2.1. Subjects

This study was approved by the Human Research Ethics Committees of the Griffith University and the Gold Coast University Hospital where scanning was performed. Patients and healthy controls were recruited over a 1-year period. Signed informed consent was obtained from all participants. The Fukuda diagnostic criteria (Fukuda et al., 1994) were used to determine the existence of CFS. The MRI scans from 83 subjects were acquired. Seven of these were excluded because they were taking medication other than paracetamol or oral contraceptive. Also excluded were four subjects with some symptoms of CFS but who did not meet the full Fukuda selection criteria, and two subjects whose body mass index (BMI) was higher than 35. The total number of subjects analysed in this study was 70, comprised of 43 CFS patients and 27 healthy controls.

2.2. MRI scans

MRI scans were acquired on a Siemens 3T Skyra with a 64 channel receive head-neck coil. We acquired T1-weighted spin echo (T1wSE) with TR/TE/flip angle = 600 ms/6.4 ms/90° and Siemens T2 'SPACE' optimized 3D fast spin-echo (T2wSE) 3200/563/variable flip angle scans. Acquisition times (min:sec) were 8:52 and 5:44. The T2wSE scans employed an optimized variable flip angle sequence (Siemens SPACE) to yield a 'true 3D' acquisition in a shortened time. Their 'contrast equivalent' TE compares with standard T2wSE TE (Busse et al., 2006), although the signal is also influenced by T1 relaxation (Mugler III, 2014), possibly more than usual.

T2wSE images were sagittal with pixel size 0.88 × 0.88 x 0.9 mm. The T1wSE were axial with voxel size 0.86 × 0.86 × 3.0 mm. A resting state fMRI and a task fMRI, each of 15 minutes duration, were also acquired and have been reported elsewhere (Shan et al., 2018a; Shan et al., 2018b). The T2wSE was acquired before the two fMRI scans and the T1wSE was acquired after them. Because the increased blood volume associated with a task stimulus lasts only a few seconds (Shan et al., 2014) the task fMRI should not influence the subsequent T1wSE signal levels.

2.3. Image processing

SPM12 (www.fil.ion.ucl.ac.uk/spm) was used to perform all voxel-based pre-processing and statistical analysis. First, the T2wSE brain images were segmented into grey matter, white matter and cerebrospinal fluid (CSF). Non-linear spatial normalization of the grey and white partitions was then optimized using DARTEL on the WM partition. An additional affine transformation of the final DARTEL grey matter template to the standard MNI grey matter template was computed and applied to the spatially normalized partitions for each subject. T1wSE images of each subject were coregistered to their raw T2wSE images and then subjected to the same deformations to MNI space. Finally, the normalised T1wSE, T2wSE and GM and WM volume images were smoothed using a 5x5x5 mm FWHM Gaussian kernel. The GM and WM partitions were further processed for voxel-based morphometry (VBM). For each subject, total GM, total WM and total intracranial volume (TIV) were computed. TIV was included as the global covariate in the VBM statistical designs.

2.4. Global normalization of MRI signal levels

T1wSE and T2wSE signal levels were normalised using the voxel-based iterative sensitivity (VBIS) method of Abbott et al (Abbott et al., 2009). VBIS requires an initial CFS group comparison with healthy controls for T1wSE (or T2wSE) images scaled using their whole-brain means (SPM's 'proportional scaling'). A mask was then defined containing those voxels with residual inter-subject variance less than the whole-brain median. A Matlab (The Mathworks Inc, Natick, MA) script was written for this purpose. The mean in this VBIS mask was then computed for each image and used as a nuisance covariate in subsequent SPM statistical designs, effectively normalising each image to a common global value. To exclude possible bias in individual analyses, a second iteration of VBIS omitted voxels from the mask where CFS vs healthy control differences (positive and negative) with uncorrected voxel $P < 0.05$ were detected. We used a 0.05 voxel threshold instead of the cluster-forming 0.001 to exclude more voxels and better minimise the bias. We only applied the second iteration to a group design

which detected large clusters, for which VBIS means could be affected by a bias introduced by any group differences within the mask. Reference to T1wSE or T2wSE signals hereafter apply to the VBIS normalized signal levels.

2.5. Voxel-wise statistical analysis

SPM12 cluster statistical inference (Hayasaka and Nichols, 2003) was used here to test for MRI group differences. Before statistical analysis, images were 'explicitly' masked with SPM12's 'mask_ICV' to exclude extra-cerebral structures. No threshold masking was used. The significance of inter-group differences was tested using family wise error (FWE) corrected cluster P value (P_{FWE}) < 0.05 with a cluster-forming threshold of voxel $P = 0.001$ (Hayasaka and Nichols, 2003).

2.6. ROI analysis

SPM group comparisons that yield multiple significant clusters do not inform about possible correlations between signal levels in those clusters in individual subjects. Tests for correlations were performed by computing median signal levels in regions-of-interest (ROIs) for individual subjects. ROIs were defined by the extent of clusters from the SPM statistical analyses (uncorrected voxel P < 0.001). A locally written Matlab script computed the median T1wSE signal level in each ROI. Regressions to test for correlations between the two ROIs were then performed using SPSS22 (IBM, New York) for both groups. Data for individual subjects were plotted with Matlab with linear fits from its 'polyfit' function.

3. Results

TIV, GM and WM volumes did not differ significantly between CFS and healthy controls. TIV (GM + WM + CSF) were 1.394 ± 0.152 L (mean ± SD) for CFS and 1.425 ± 0.134 L for healthy controls; GM volumes were 0.623 ± 0.072 L and 0.660 ± 0.092 L; WM volumes were 0.511 ± 0.068 L and 0.516 ± 0.058 L.

3.1. T1wSE group comparisons

The regions used to compute T1wSE global means for the first and second VBIS iterations are shown in Fig. 1A and B. All T1wSE results reported herein are from the second iteration analysis. The T1wSE group comparison revealed signal *increases* in CFS in a large cluster involving mostly gyral WM of the premotor, primary motor and primary sensory cortex (Figs. 1C, 2, Table 1), although there was also some GM involvement. This cluster also extended into the somatosensory cortex with foci in BA5 and BA7 and into the cingulate cortex. This large cluster was highly significant ($P_{FWE} < 0.0001$). The peak voxel (voxel $P_{FWE} = 0.04$) at (-33 -36 57) was located in WM of the hand area of the primary sensory cortex. When low level voxels were excluded from analysis by setting SPM's 'relative threshold masking' to 0.6 x mean signal level, the merged cluster separated into left and right clusters with $P_{FWE} < 0.0001$ for both. Improved spatial localisation was achieved by imposing a stricter cluster forming threshold of 0.00002. This yielded five significant clusters in gyral WM, two located in the primary sensory cortex with peaks at (-33 -36 57) and (16 -39 69) and three in the primary motor cortex (8 -28 60), (-6 -18 70) and (12 -15 70).

The T1wSE group comparison also revealed *decreases* in CFS in a cluster ($P_{FWE} = 0.002$) extending through the brainstem (Fig. 3, Table 1). This cluster included the posterior hypothalamus (Fig. 3, z = -8, x = 0), ventral tegmental area (VTA) (z = -14, x = 0) and pontine nuclei (z = -26, x = -6).

The T1wSE group comparison adjusted with global means from the second iteration of VBIS slightly strengthened the statistical inference for CFS > healthy controls (HC) and weakened it for CFS < HC, relative to the first iteration.

3.2. T1wSE correlation between brainstem and cortex

Looking beyond the group differences in T1wSE, we ask: are signal *increases* in individuals related to their signal *decreases*? To answer this we performed regression analysis over individual subjects between median T1wSE signal levels in a region defined by the merged left and right sensorimotor cluster and a region defined by the brainstem cluster. We found very significant negative correlations for both CFS ($R^2 = 0.31$, $P = 0.00007$) and healthy controls ($R^2 = 0.34$, $P = 0.0009$), see Fig. 4 and Table 2. While 'b', the slope, was less steep for CFS than for healthy controls, their 95% confidence levels overlapped. The correlation was even stronger when CFS and healthy controls (HC) were

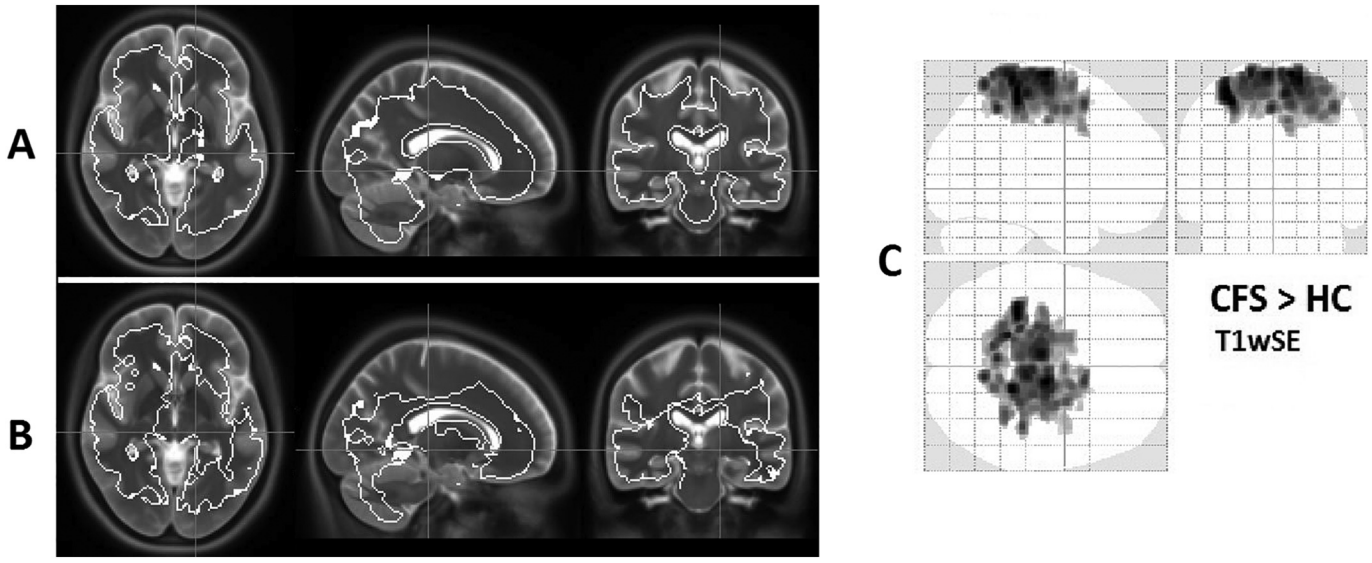

Fig. 1. A. Edges of the VBIS mask used to evaluate global means in individual CFS and healthy control (HC) T1wSE scans, shown on the average T2wSE image from this study. WM areas dominate. B. Edges of second iteration VBIS mask after excluding voxels where for T1wSE, CFS > HC or CFS < HC (uncorrected voxel P < 0.05) adjusted with global values from mask A. Exclusions are clear in sensorimotor, brainstem, cerebellum and right insula areas (see *). C. Maximum T-statistic Projection Maps for CFS > healthy controls (HC) for T1wSE with a voxel P threshold of 0.001 adjusted with global values from mask B.

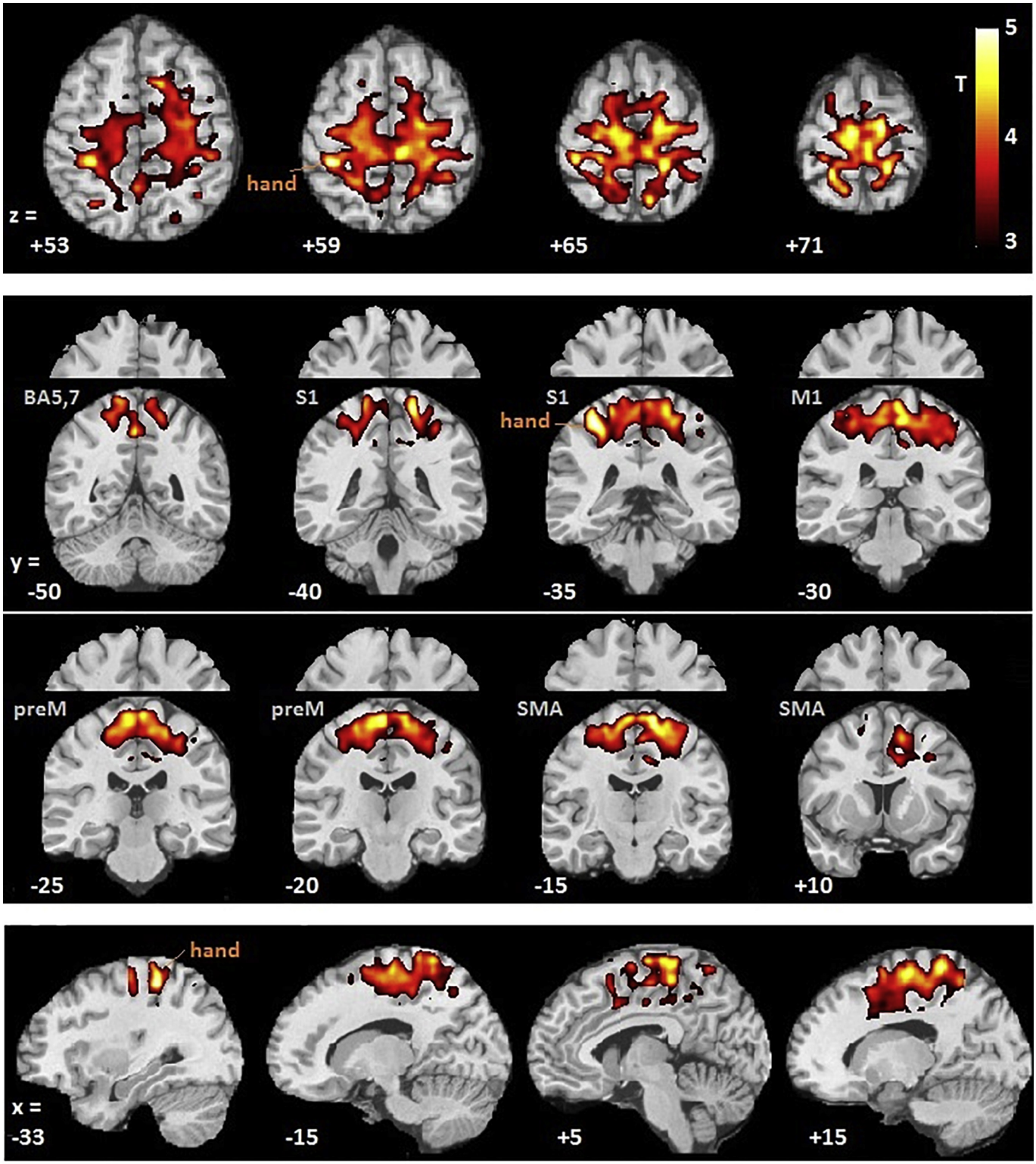

Fig. 2. Thresholded ($p < 0.001$) SPM T maps (red-yellow) indicating T1wSE signal higher in CFS than in healthy controls. Axial, coronal and sagittal sections through the cluster in Fig. 1 are superimposed on reference brain sections. Increases occur mostly in gyral white matter although there is also some adjacent grey matter involvement. The most significant voxel (see x = -35, y = -35, z = -33) is in the hand area of S1. The gyral locations in the coronal sections are labelled as 'BA5,7' somatosensory cortex, 'S1' primary somatosensory, 'M1' primary motor, 'preM' premotor and 'SMA' supplementary motor area. Blank reference coronal sections are included to assist visual separation of grey matter and white matter.

pooled (R^2 = -0.44). Slopes of the regressions were near unity (-1.06 for HC and -0.96 for CFS + HC), suggesting similar factors influence T1wSE in the brainstem and in the sensorimotor cortex. In Fig. 4 the relative CFS and HC signal amplitudes differ as expected from their group comparisons. The overall signal levels also differ, from a mean of 809 for the sensorimotor areas to 1124 for the brainstem, indicating a difference in MRI receiver coil sensitivity between the two areas (this is not the same as SNR).

Table 1
Cluster statistics for group comparisons of CFS with healthy controls. The voxel *P* threshold for cluster formation was 0.001. Cluster P_{FWE}: FWE corrected cluster *P*, L+R: left+right. Voxel dimension was 1.5x1.5x1.5 mm.

T1wSE	Cluster P_{FWE}	Cluster size	Location	Peak voxel
CFS > healthy controls	< .0001	16336	L+R sensorimotor	-33 -36 57
CFS < healthy controls	0.002	1025	brainstem	-15 -24 -40

3.3. T2wSE, GM volume, WM volume analysis

Group comparisons of the T2wSE, GM volume and WM volume images showed no significant clusters. However, for T2wSE when the cluster forming voxel *P* threshold was relaxed from 0.001 to 0.005, three significant clusters for CFS > Healthy Controls were detected in sensorimotor WM.

4. Discussion

There were three main results, all from the group comparison of T1wSE scans:

A. We detected *decreased* signal-levels in the brainstem in CFS (Fig. 3) relative to healthy controls. The cluster extended over the ventral tegmental area (VTA) and posterior hypothalamus (pHT) through pontine nuclei to the medulla. Brainstem white matter volume losses have been observed in CFS with some VBM studies (Barnden et al., 2011; Finkelmeyer et al., 2018), but not here.
B. We detected *increased* signal-levels in CFS in gyral white matter of the sensorimotor cortex where projection fibres from the thalamus terminate (Wacana et al., 2004) (Fig. 1C, 2). This complements previously observed severity dependent *increased* myelination low in the same fibres in the internal capsule (Barnden et al., 2015).

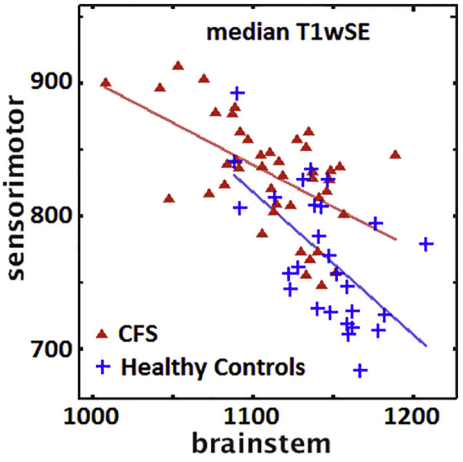

Fig. 4. Individual-subject median T1wSE signal levels in the sensorimotor region plotted against median levels from the brainstem region. The correlation R^2 and null probability were 0.32 and P = 0.00007 for CFS, and 0.34 and 0.0009 for Healthy Controls (HC). Linear fits to the data are shown for CFS (red) and HC (blue). The CFS and HC slopes were not significantly different (Table 2). Individual subject T1wSE signals were normalized to a global mean of 1000 using VBIS derived global values. CFS sensorimotor T1wSE values are mostly higher, and CFS brainstem T1wSE mostly lower, than Healthy Control values as expected from the group analysis results. Normalized T1wSE values were generally higher for the brainstem (near 1100) than for the sensorimotor region (near 800), indicating a difference in receiver coil sensitivity between them.

C. A strong negative correlation was detected between signal levels from the brainstem and sensorimotor WM for both CFS and healthy controls (Fig. 4, Table 2). To our knowledge this is a novel finding in both healthy controls and CFS.

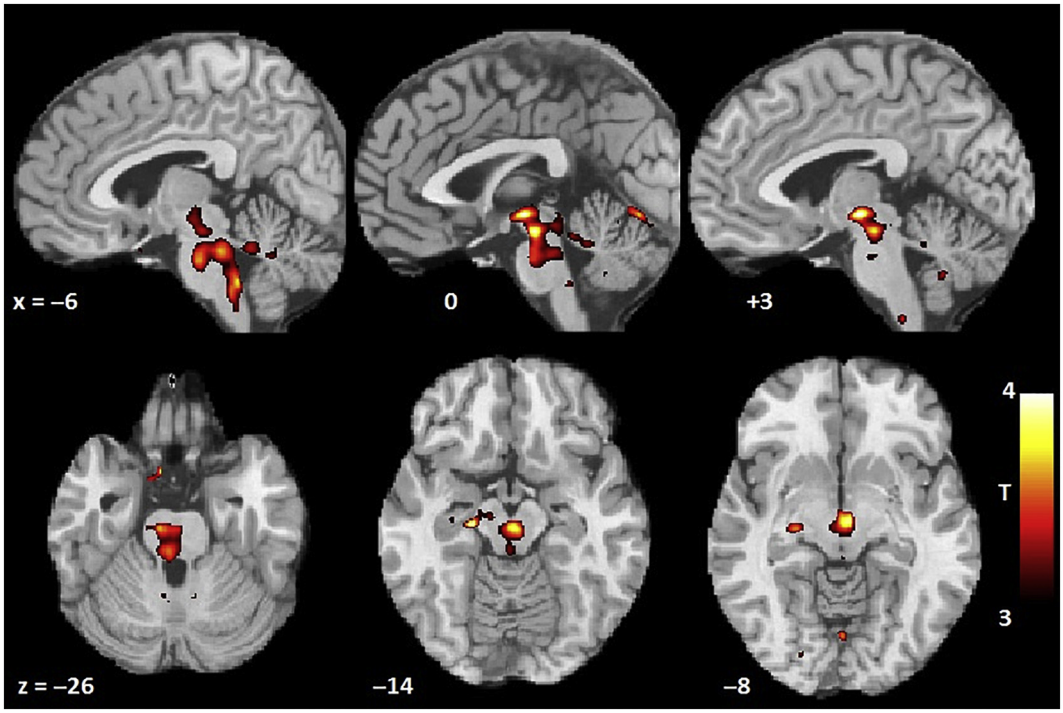

Fig. 3. Thresholded (p < 0.001) SPM T maps (coloured) indicating T1wSE signal lower in CFS than healthy controls superimposed on a reference brain. Sections of a single brainstem cluster through the midbrain, pons and medulla are shown. Foci occur in the posterior hypothalamus (z=-8, x=0), ventral tegmental area (z=-14, x=0), pontine nuclei (z=-26, x=-6) and reticular formation nuclei in the medulla (z=-26, x=-6).

Table 2
Linear regression y = bx + c for median sensorimotor (y) versus brainstem (x) normalized T1wSE levels (Fig. 4) from separate regressions for the CFS group, the Healthy Controls (HC) and both groups pooled (CFS + HC). Regions were defined by the CFS > HC and CFS < HC clusters in Table 1.

Cohort	N	Slope b	95% confidence	Intercept c	95% confidence	R^2	*P*
CFS	43	-0.63	-0.91, -0.34	1530	1210, 1850	0.31	0.00007
HC	27	-1.06	-1.64, -0.48	1990	1330, 2650	0.34	0.0009
CFS + HC	70	-0.96	-1.21,-0.70	2170	1590, 2170	0.44	3e-10

4.1. T1wSE signals

MRI signals are modulated by the tissue dependent relaxation times T1 and T2. The amplitude of MRI signals is primarily influenced by the local relaxation rates R1 (1/T1) and R2 (1/T2). Both are dependent on local iron concentration [Fe], and macromolecular mass fraction. A combination of the two was shown to explain T1 variations in the brain (Rooney et al., 2007) in both GM and WM for 0.2T – 7T MRI. Myelin makes up 50% by dry weight of macromolecular mass in WM, although the relative contribution of myelin concentration [myelin], to T1 and T2 contrast has been contentious. Stuber et al (Stuber et al., 2014) applied proton induced X-Ray emission to spatially resolve the distribution and concentration of iron, phosphorus and sulphur in cortical brain samples fixed 36 hours postmortem. This yielded [Fe] directly and the phosphorus and sulphur concentrations were used to specifically compute [myelin], as distinct from macromolecule concentration measured by earlier staining methods. They demonstrated that R1 and R2* could be modelled by the sum of two terms, the first linearly dependent on [myelin] and the second linearly dependent on [Fe]. The portion of R1 contrast determined by [myelin] was 90% in WM and 64% in GM. [Fe] accounted for the remainder. Therefore, there is now greater confidence that [myelin] dominates T1 MRI contrast in WM.

4.2. Brainstem T1wSE decreases

Although it may be reasonable to attribute changes in T1wSE in sensorimotor WM to changes in myelin levels, in the brainstem this is problematic because of interspersed gray matter. The brainstem contains multiple small and dispersed neuron structures in reticular formations in the midbrain, pons and medulla, as well as other autonomic and neurohormonal centres. Brainstem T1wSE changes could therefore reflect changes in this complex dispersed GM which could involve changes in levels of [Fe] or macromolecules other than myelin. Brainstem inflammation in CFS (Nakatomi et al., 2014), if accompanied by some oedema, would also reduce T1wSE signals. On the other hand, the near unity slope of the brainstem vs sensorimotor regression supports a common source for the T1wSE changes.

The CFS group differences in brainstem T1wSE reported here (A above) were not seen in an earlier study (Barnden et al., 2011). However, that study did detect an abnormal regression of an autonomic measure (pulse pressure) with T1wSE in a brainstem area similar to that in (B) which was consistent with impaired connectivity between brainstem regulatory nuclei. Factors contributing to the novel detection of a brainstem T1wSE decrease here (A above) include a possible improvement in brainstem SNR, spatial normalization based on the T2wSE scan with its spin-echo resistance to distortion, optimization of spatial normalization using the WM partition instead of GM, and greater subject numbers.

4.3. Sensorimotor T1wSE increases

T1wSE signal levels are primarily influenced by T1 relaxation rates. In WM, 90% of T1 contrast is determined by myelin concentration (Stuber et al., 2014) and we refer to myelination or myelin level below instead of T1wSE signal level in sensorimotor WM. The increase in myelination (B above) in extended gyral WM of the premotor, primary motor (M1), primary somatosensory (S1) and nearby somatosensory areas (Fig. 2) had strong cluster significance (Table 1). A significant focus was seen in the hand area of S1 (peak *voxel* P_{FWE} = 0.04). *Increased* motor network connectivity has been observed in Parkinson's Disease (PD) (Baudrexel et al., 2011; Wu et al., 2009), suggesting myelin between the thalamus and motor cortex may be upregulated in PD. It was striking that the strongest increase in connectivity in the PD study (Baudrexel et al., 2011) was also found to the hand area of S1 (and M1). Thalamocortical connectivity was also enhanced in the severe epilepsy of Lennox-Gastaut syndrome (Warren et al., 2017). Although we do not report directly on sensorimotor connectivity here, increased myelin levels would be expected to enhance it.

The high gyral/cortical SNR of the MRI multichannel head-neck coil used here is the most likely reason we discovered the extended increase in myelination in CFS in WM of the sensorimotor cortex. The earlier study which failed to detect this difference (Barnden et al., 2011) was performed on 1.5T system with a SNR near 70 (Maubon et al., 1999), less than the cortical SNR near 350 for the 3T system here (Keil et al., 2013). Although the high surface SNR here extends evenly over the whole cortical surface the steep decrease in SNR with depth (Keil et al., 2013) means myelin increases may extend deeper for the full length of projection fibres, but be undetectable with this instrumentation.

4.4. Inverse correlation between sensorimotor and brainstem T1wSE

The negative regression (C above) detected between T1wSE in the brainstem and sensorimotor regions (Fig. 4, Table 2) was similar for both CFS and healthy controls. The mechanism that drives these relationships is therefore likely to be the same for the two groups. The regression slope for the healthy control group was negative and near unity (Table 2) suggesting that in healthy humans, brainstem-to-sensorimotor connectivity is maintained by balancing the same 'conduction factor' such that a smaller brainstem factor is accompanied by a larger sensorimotor factor and vice versa. Myelination is an obvious candidate for such a 'conduction factor'. If so, it raises the possibility that in CFS, elevated sensorimotor myelination is stimulated by depleted brainstem myelination. There is indirect evidence for impaired connectivity within the brainstem in CFS (Barnden et al., 2016) and this would affect multiple motor circuits in the brain (see below). While the nature of this putative sensorimotor stimulatory mechanism is unknown, it conceivably maintains a critical level of connectivity between the brainstem and sensorimotor cortex in order to maintain an adequate level of motor performance.

Ascending fibres from the brainstem pass to the sensorimotor area via the thalamus. Thalamo-cortical connections act in two directions. There are both projection fibres from the thalamus to the cortex and (many more) regulatory fibres returning back to essentially the same area of the thalamus (Hall, 2011; Nolte, 2002). Projection fibres are subject to regulation of myelination to maintain constant signal latency between the thalamus and cortex (Salami et al., 2003). Inputs via the brainstem to the thalamus that pass via projection fibres to the motor and/or sensory cortex include: ascending fibres that return somatosensory information from a muscle activated by the motor cortex, and fibres from the accessory motor systems of the basal ganglia and cerebellum which receive input from the motor cortex. All pass through one or more sections of the brainstem (mid brain, pons and medulla) to the thalamus. Therefore, motor functions that may drive maintenance of brainstem-to-cortex signalling include return of somatosensory information to the cortex, conscious motor function and subconscious learned patterns of movement (basal ganglia), and planning and coordination of rapid and forceful muscle movements (cerebellum) (Hall, 2011).

Although the known plasticity of projection fibres makes them a candidate for upregulated sensorimotor myelination, it is not known whether upregulation may affect other fibres. Does it also involve descending regulatory fibres to the thalamus and/or descending motor (cortico-spinal, cortico-bulbar, cortico-cerebellar) fibres and/or collateral fibres between adjacent cortical areas?

Reports in CFS of brainstem neuroinflammation (Nakatomi et al., 2014) and implicit impairment of intra-brainstem connectivity (Barnden et al., 2016), together with known thalamo-cortical myelin plasticity (Salami et al., 2003), suggest that the inverse relationship observed here between brainstem T1wSE changes and sensorimotor gyral WM myelin is most likely driven by changes in the brainstem. That is, in CFS, brainstem connectivity deficits compromise ascending signals to stimulate the mechanism illustrated in Fig. 4 to amplify distal thalamo-cortical myelination and thereby maintain brainstem-to-cortex connectivity. We had invoked such a mechanism in CFS earlier (Barnden et al., 2015) to interpret severity dependent internal capsule myelin upregulation. If the lower regression slope for CFS in Fig. 4 is eventually shown to be significant, it would suggest that compensation in sensorimotor WM for impaired brainstem conduction was not fully achieved, as is suggested by prolonged motor conduction times in CFS (Hilgers et al., 1998).

4.5. Can variable receiver coil sensitivity explain the negative correlation?

The raw T1wSE images exhibited a smoothly varying fall off in signal from the brain centre to the sensorimotor cortex of about 30% (see Fig S1 in Supplementary material and Fig. 4 axes). No correction for this was attempted. To test whether this variation in receiver coil sensitivity might explain the inverse correlation in Fig. 4 between brainstem and motor cortex ROI levels, we evaluated three arbitrary gyral WM ROIs and one GM ROI in the frontal pole where sensitivity was also reduced (see Supplementary Material). No systematic correlations with the brainstem ROI signal were found and we dismissed variability in T1wSE receiver coil sensitivity as a contributor to the negative brainstem versus sensorimotor cortex correlations.

4.6. Technical implications

This study highlights the usefulness of the high SNR, low distortion T1wSE scan in clinical studies. The dependence of these scans on myelin in WM can provide valuable insights in clinical cross-sectional and longitudinal studies.

4.7. Limitations

We interpreted T1wSE change in WM as myelin density change. This is the most likely explanation in WM of the sensorimotor area (Stuber et al., 2014) although changes to levels of other macromolecules or iron (ferritin) may be relevant in the brainstem. Because the statistical inference here was for clusters of voxels, uncertainty exists about which brainstem WM tracts or nuclei may be relevant to the associated CFS sensorimotor changes in T1wSE/myelination. The possibility of some T1wSE contrast deriving from T2 and proton density as well as T1 could be resolved by using pure T1 imaging such as is generated by MP2RAGE sequences, although whether their SNR and subject-to-subject accuracy is adequate for voxel based cross-sectional studies needs to be established. Our conclusion that brainstem deficits reduce brainstem connectivity and stimulate elevated sensorimotor myelin needs to be confirmed and clarified by fMRI connectivity and diffusion MRI studies.

5. Conclusions

In CFS T1wSE was elevated in sensorimotor WM and decreased in the brainstem. In both healthy controls and CFS, T1wSE (myelination) in sensorimotor WM showed the same inverse correlation with T1wSE in the brainstem. This relationship, previously unreported in either healthy controls or CFS, suggested a possibility that in CFS a normal regulatory mechanism had responded to impaired brainstem signal conduction to stimulate elevated sensorimotor myelination. This complements evidence in CFS for severity dependent myelin upregulation in the internal capsule (Barnden et al., 2015). Deficits in brainstem function in CFS can have broad consequences for regulation of cerebral function in general and myelination in particular and should be a focus of future research in CFS.

Supplementary data to this article can be found online at https://doi.org/10.1016/j.nicl.2018.07.011.

Acknowledgements

We thank the patients and healthy controls who donated their time and effort to participate in this study. This study was supported by the Stafford Fox Medical Research Foundation, the Judith Jane Mason Foundation (MAS2015F024), Mr Douglas Stutt, and the Blake-Beckett Foundation. The financial support did not affect any aspect of the study.

References

Abbott, D., Pell, G., Pardoe, H., Jackson, G., 2009. Voxel-Based Iterative Sensitivity (VBIS): methods and a validation of intensity scaling for T2-weighted imaging of hippocampal sclerosis. NeuroImage. 44, 812–819.

Barnden, L., Crouch, B., Kwiatek, R., Burnet, R., Mernone, A., Chryssidis, S., et al., 2011. A brain MRI study of chronic fatigue syndrome: Evidence of brainstem dysfunction and altered homeostasis. NMR Biomed. 24 (10), 1302–1312.

Barnden, L., Crouch, B., Kwiatek, R., Burnet, R., Del Fante, P., 2015. Evidence in Chronic Fatigue Syndrome for severity-dependent upregulation of prefrontal myelination that is independent of anxiety and depression. NMR Biomed. 28 (3), 404–413.

Barnden, L., R, K., Crouch, B., Burnet, R., Del Fante, P., 2016. Autonomic correlations with MRI are abnormal in the brainstem vasomotor centre in Chronic Fatigue Syndrome. NeuroImage 11, 530–537.

Baudrexel, S., Witte, T., Seifried, C., von Wegner, F., Beissner, F., Klein, J.C., et al., 2011. Resting state fMRI reveals increased subthalamic nucleus-motor cortex connectivity in Parkinson's disease. Neuroimage. 55 (4), 1728–1738.

Boissoneault, J., Letzen, J., Lai, S., O'Shea, A., Craggs, J., Robinson, M.E., et al., 2016a. Abnormal resting state functional connectivity in patients with chronic fatigue syndrome: an arterial spin-labeling fMRI study. Magnetic Resonance Imaging. 34 (4), 603–608.

Boissoneault, J., Letzen, J., Lai, S., Robinson, M.E., Staud, R., 2016b. Static and dynamic functional connectivity in patients with chronic fatigue syndrome: use of arterial spin labelling fMRI. Clin. Physiol. Funct. Imag. 38, 128–137.

Busse, R.F., Hariharan, H., Vu, A., Brittain, J.H., 2006. Fast spin echo sequences with very long echo trains: design of variable refocusing flip angle schedules and generation of clinical T2 contrast. Magnetic Resonance Med. 55 (5), 1030–1037.

Carruthers, B., van de Sande, M., DeMeirleir, K., Klimas, N., Broderick, G., Mitchell, T., et al., 2011. Myalgic encephalomyelitis: International Consensus Criteria. J Intern Med. 270, 327–338.

Caseras X, Mataix-Cols D, Rimes K, Giampietro V, M. Brammer M, Zelaya F, et al. The neural correlates of fatigue: an exploratory imaginal fatigue provocation study in chronic fatigue syndrome. Psychol Med. 2008;38:941-51.

Cook, D., O'Connor, P., Lange, G., Steffener, J., 2007. Functional neuroimaging correlates of mental fatigue induced by cognition among chronic fatigue syndrome patients and controls. NeuroImage. 36, 108–122.

de Lange, F., Kalkman, J., Bleijenberg, G., Hagoort, P., Sieberen, P., van der Werf, S., et al., 2004. Neural correlates of the chronic fatigue syndrome - an fMRI study. Brain. 127, 1948–1957.

Finkelmeyer, A., He, J., Maclachlan, L., Watson, S., Gallagher, P., Newton, J.L., et al., 2018. Grey and white matter differences in Chronic Fatigue Syndrome - A voxel-based morphometry study. NeuroImage Clinical. 17, 24–30.

Fukuda, K., Straus, S.E., Hickie, I., Sharpe, M.C., Dobbins, J.G., Komaroff, A., 1994. The chronic fatigue syndrome: a comprehensive approach to its definition and study. Ann Intern Med. 121, 953–959.

Gay, C.W., Robinson, M.E., Lai, S., O'Shea, A., Craggs, J.G., Price, D.D., et al., 2016. Abnormal Resting-State Functional Connectivity in Patients with Chronic Fatigue Syndrome: Results of Seed and Data-Driven Analyses. Brain connectivity. 6 (1), 48–56.

Hall, J., 2011. Guyton and Hall Textbook of Physiology. Elsevier, Philadelphia: Saunders.

Hayasaka, S., Nichols, T.E., 2003. Validating cluster size inference: random field and permutation methods. Neuroimage. 20 (4), 2343–2356.

Hilgers, A., Frank, J., Bolte, P., 1998. Prolongation of central motor conduction time in chronic fatigue syndrome. J Chronic Fatigue Synd. 4 (2), 23–32.

Keil, B., Blau, J.N., Biber, S., Hoecht, P., Tountcheva, V., Setsompop, K., et al., 2013. A 64-channel 3T array coil for accelerated brain MRI. Magnetic resonance in medicine. 70 (1), 248–258.

Kim, B.H., Namkoong, K., Kim, J.J., Lee, S., Yoon, K.J., Choi, M., et al., 2015. Altered

resting-state functional connectivity in women with chronic fatigue syndrome. Psychiatry Res. 234 (3), 292–297.
Lange, G., Steffener, T., Cook, D., Bly, B., Christodoulou, C., Liu, W.-C., et al., 2005. Objective evidence of cognitive complaints in Chronic Fatigue Syndrome: A BOLD fMRI study of verbal working memory. NeuroImage. 26, 513–524.
Maubon, A.J., Ferru, J.M., Berger, V., Soulage, M.C., DeGraef, M., Aubas, P., et al., 1999. Effect of field strength on MR images: comparison of the same subject at 0.5, 1.0, and 1.5 T. Radiographics 19 (4), 1057–1067.
Mizuno, K., Tanaka, M., Tanabe, H.C., Joudoi, T., Kawatani, J., Shigihara, Y., et al., 2015. Less efficient and costly processes of frontal cortex in childhood chronic fatigue syndrome. NeuroImage Clinical. 9, 355–368.
Mizuno, K., Kawatani, J., Tajima, K., Sasaki, A.T., Yoneda, T., Komi, M., et al., 2016. Low putamen activity associated with poor reward sensitivity in childhood chronic fatigue syndrome. NeuroImage Clinical. 12, 600–606.
Mugler III, J.P., 2014. Optimized three-dimensional fast-spin-echo MRI. J Magn Reson Imaging. 39 (4), 745–767.
Nakatomi, Y., Mizuno, K., Ishii, A., Wada, Y., Tanaka, M., Tazawa, S., et al., 2014. Neuroinflammation in Patients with Chronic Fatigue Syndrome/Myalgic Encephalomyelitis: An 11C-(R)-PK11195 PET Study. J Nucl Med. 55, 945–950.
Nolte, J., 2002. The Human Brain. An Introduction to its Functional Anatomy, 5th ed. Mosby, St. Louis.
Rooney, W.D., Johnson, G., Li, X., Cohen, E.R., Kim, S.G., Ugurbil, K., et al., 2007. Magnetic field and tissue dependencies of human brain longitudinal 1H2O relaxation in vivo. Magnetic Resonance in Medicine. 57 (2), 308–318.
Salami, M., Itami, C., Tsumoto, T., Kimura, F., 2003. Change of conduction velocity by regional myelination yields constant latency irrespective of distance between thalamus and cortex. Proc Nat Accad Sci. 100, 6174–6179.
Shan, Z., Wright, M., Thompson, P., McMahon, K., Blokland, G., de Zubicaray, G., et al., 2014. Modeling of the Hemodynamic Responses in Block Design fMRI Studies. J Cereb Blood Flow & Metab. 34, 316–324.
Shan, Z.Y., Finegan, K., Bhuta, S., Ireland, T., Staines, D.R., Marshall-Gradisnik, S.M., et al., 2018a. Decreased connectivity and increased blood oxygenation level dependent complexity in the default mode network in individuals with chronic fatigue syndrome. Brain Connectivity. 8 (1), 33–39.
Shan, Z., Finegan, K., Bhuta, S., Ireland, T., Staines, D., Marshall-Gradisnik, S., et al., 2018b. Brain function characteristics of chronic fatigue syndrome: a task fMRI study. NeuroImage Clinical. 19, 279–286.
Stuber C, Morawski M, Schafer A, Labadie C, Wahnert M, Leuze C, et al. Myelin and iron concentration in the human brain: a quantitative study of MRI contrast. Neuroimage. 2014;93 Pt 1:95-106.
Tanaka, M., Sadato, N., Okada, T., Mizuno, K., Sasabe, T., Tanabe, H.C., et al., 2006. Reduced responsiveness is an essential feature of chronic fatigue syndrome: a fMRI study. BMC Neurol. 6, 9.
Wacana, S., Jiang, H., Nagae-Poetscher, L., van Zijl, P., Mori, S., 2004. Fiber tract-based atlas of human white matter anatomy. Radiology. 230, 77–87.
Warren, A.E.L., Abbott, D.F., Jackson, G.D., Archer, J.S., 2017. Thalamocortical functional connectivity in Lennox-Gastaut syndrome is abnormally enhanced in executive-control and default-mode networks. Epilepsia. 58 (12), 2085–2097.
Wortinger, L.A., Endestad, T., Melinder, A.M., Oie, M.G., Sevenius, A., Bruun Wyller, V., 2016. Aberrant Resting-State Functional Connectivity in the Salience Network of Adolescent Chronic Fatigue Syndrome. PLoS One. 11 (7), e0159351.
Wortinger, L.A., Glenne Oie, M., Endestad, T., Bruun Wyller, V., 2017. Altered right anterior insular connectivity and loss of associated functions in adolescent chronic fatigue syndrome. PLoS One. 12 (9), e0184325.
Wu, T., Wang, L., Chen, Y., Zhao, C., Li, K., Chan, P., 2009. Changes of functional connectivity of the motor network in the resting state in Parkinson's disease. Neuroscience Letters. 460 (1), 6–10.